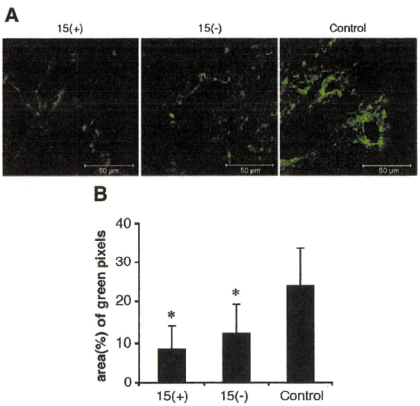

Fig. 6. Antiangiogenic effect of expressed sFlt-1 in BxPC3 tumor bearing mice. Tumor microvessels were detected by CD31 (PECAM1) antibody staining of tumor cryosections 20 days after therapy. (A) Representative CD31 immunostaining images. (B) Quantitative analysis of microvessel density in tumor cryosections. The results represent a percentage area of green pixels per image. Seven images were taken from each tumor tissue, from 3 mice, mean ± s.d. *$P<0.05$ compared to control group.

Science and Technology Agency (JST) as well as by Grants-in-Aid for Young Scientists (A). We express our appreciation to Prof. M. Shibuya (Tokyo Medical and Dental University) for providing pVL 1393 baculovirus vector pDNA encoding human sFlt-1. We thank Ms. S. Ogura (The University of Tokyo) for her technical assistance.

References

[1] A. Harada, K. Kataoka, Formation of polycation complex micelles in an aqueous milieu from a pair of oppositely-charged block copolymers with poly(ethylene glycol) segments, Macromolecules 28 (15) (1995) 5294–5299.
[2] S. Katayose, K. Kataoka, Water-soluble polyion complex associates of DNA and poly(ethylene glycol)-poly(L-lysine) block copolymer, Bioconjug. Chem. 8 (5) (1997) 702–707.
[3] M. Harada-Shiba, K. Yamauchi, A. Harada, I. Takamisawa, K. Shimokado, K. Kataoka, Polyion complex micelles as vectors in gene therapy – pharmacokinetics and in vivo gene transfer, Gene Ther. 9 (6) (2002) 407–414.
[4] M. Laus, K. Sparnacci, B. Ensoli, S.O. Buttò, A. Caputo, I. Mantovani, G. Zuccheri, B. Samorì, L. Tondelli, Complex associates of plasmid DNA and a novel class of block copolymers with PEG and cationic segments as new vectors for gene delivery, J. Biomater. Sci. Polym. Ed. 12 (2) (2001) 209–228.
[5] C.H. Ahn, S.Y. Chae, Y.H. Bae, S.W. Kim, Synthesis of biodegradable multi-block copolymers of poly(L-lysine) and poly(ethylene glycol) as a non-viral gene carrier, J. Control. Release 97 (3) (2004) 567–574.
[6] Y. Wang, C.Y. Ke, B.C. Weijie, S.Q. Liu, S.H. Goh, Y.Y. Yang, The self-assembly of biodegradable cationic polymer micelles as vectors for gene transfection, Biomaterials 28 (35) (2007) 5358–5368.
[7] Y.R. Choi, S.Y. Chae, C.H. Ahn, M. Lee, S. Oh, Y. Byun, B.D. Rhee, K.S. Ko, Development of polymeric gene delivery carriers: PEGylated copolymers of L-lysine and L-phenylalanine, J. Drug Target. 15 (6) (2007) 391–398.
[8] K. Itaka, K. Yamauchi, A. Harada, K. Nakamura, H. Kawaguchi, K. Kataoka, Polyion complex micelles from plasmid DNA and poly(ethylene glycol)-poly(L-lysine) block copolymer as serum-tolerable polyplex system: physicochemical properties of micelles relevant to gene transfection efficiency, Biomaterials 24 (24) (2003) 4495–4506.
[9] S. Mishra, P. Webster, M.E. Davis, PEGylation significantly affects cellular uptake and intracellular trafficking of non-viral gene delivery particles, Eur. J. Cell Biol. 83 (3) (2004) 97–111.
[10] A.M. Funhoff, S. Monge, R. Teeuwen, G.A. Koning, N.M. Schuurmans-Nieuwenbroek, D.J. Crommelin, D.M. Haddleton, W.E. Hennink, C.F. van Nostrum, PEG shielded polymeric double-layered micelles for gene delivery, J. Control. Release 102 (3) (2005) 711–724.
[11] H.K. de Wolf, C.J. Snel, F.J. Verbaan, R.M. Schiffelers, W.E. Hennink, G. Storm, Effect of cationic carriers on the pharmacokinetics and tumor localization of nucleic acids after intravenous administration, Int. J. Pharm. 331 (2) (2007) 167–175.
[12] K. Miyata, Y. Kakizawa, N. Nishiyama, A. Harada, Y. Yamasaki, H. Koyama, K. Kataoka, Block catiomer polyplexes with regulated densities of charge and disulfide cross-linking directed to enhance gene expression, J. Am. Chem. Soc. 126 (8) (2004) 2355–2361.
[13] K. Miyata, Y. Kakizawa, N. Nishiyama, Y. Yamasaki, T. Watanabe, M. Kohara, K. Kataoka, Freeze-dried formulations for in vivo gene delivery of PEGylated polyplex micelles with disulfide crosslinked cores to the liver, J. Control. Release 109 (1–3) (2005) 15–23.
[14] M. Oba, S. Fukushima, N. Kanayama, K. Aoyagi, N. Nishiyama, H. Koyama, K. Kataoka, Cyclic RGD peptide-conjugated polyplex micelles as a targetable gene delivery system directed to cells possessing $\alpha_v\beta_3$ and $\alpha_v\beta_5$ integrins, Bioconjug. Chem. 18 (5) (2007) 1415–1423.
[15] M. Oba, K. Aoyagi, K. Miyata, Y. Matsumoto, K. Itaka, N. Nishiyama, Y. Yamasaki, H. Koyama, K. Kataoka, Polyplex Micelles with cyclic RGD peptide ligands and disulfide cross-links directing to the enhanced transfection via controlled intracellular trafficking, Mol. Pharmaceutics 5 (6) (2008) 1080–1092.
[16] M.D. Pierschbacher, E. Ruoslahti, Cell attachment activity of fibronectin can be duplicated by small synthetic fragments of the molecule, Nature 309 (5963) (1984) 30–33.
[17] R. Haubner, R. Gratias, B. Diefenbach, S.L. Goodman, A. Jonczyk, H. Kessler, Structural and functional aspects of RGD-containing cyclic pentapeptides as highly potent and selective integrin $\alpha_v\beta_3$ antagonists, J. Am. Chem. Soc. 118 (1996) 7461–7472.
[18] A. Erdreich-Epstein, H. Shimada, S. Groshen, M. Liu, L.S. Metelitsa, K.S. Kim, M.F. Stins, R.C. Seeger, D.L. Durden, Integrins alpha(v)beta3 and alpha(v)beta5 are expressed by endothelium of high-risk neuroblastoma and their inhibition is associated with increased endogenous ceramide, Cancer Res. 60 (3) (2000) 712–721.
[19] R.M. Schiffelers, A. Ansari, J. Xu, Q. Zhou, Q. Tang, G. Storm, G. Molema, P.Y. Lu, P.V. Scaria, M.C. Woodle, Cancer siRNA therapy by tumor selective delivery with ligand-targeted sterically stabilized nanoparticle, Nucleic Acids Res. 32 (19) (2004) e149.
[20] W.J. Kim, J.W. Yockman, M. Lee, J.H. Jeong, Y.H. Kim, S.W. Kim, Soluble Flt-1 gene delivery using PEI-g-PEG-RGD conjugate for anti-angiogenesis, J. Control. Release 106 (1–2) (2005) 224–234.
[21] W.J. Kim, J.W. Yockman, J.H. Jeong, L.V. Christensen, M. Lee, Y.H. Kim, S.W. Kim, Anti-angiogenic inhibition of tumor growth by systemic delivery of PEI-g-PEG-RGD/pCMV-sFlt-1 complexes in tumor-bearing mice, J. Control. Release 114 (3) (2006) 381–388.
[22] K. Temming, R.M. Schiffelers, G. Molema, R.J. Kok, RGD-based strategies for selective delivery of therapeutics and imaging agents to the tumor vasculature, Drug Resist. Updat. 8 (6) (2005) 381–402.
[23] K.A. Thomas, Vascular endothelial growth factor, a potent and selective angiogenic agent, J. Biol. Chem. 271 (2) (1996) 603–606.
[24] G. Breier, Functions of the VEGF/VEGF receptor system in the vascular system, Semin. Thromb. Hemost. 26 (5) (2000) 553–559.
[25] R.A. Brekken, P.E. Thorpe, VEGF-VEGF receptor complexes as markers of tumor vascular endothelium, J. Control. Release 74 (1–3) (2001) 173–181.
[26] A.L. Harris, Anti-angiogenesis therapy and strategies for integrating it with adjuvant therapy, Recent Results Cancer Res. 152 (1998) 341–352.
[27] N. Ferrara, VEGF as a therapeutic target in cancer, Oncology 69 (2005) 11–16.
[28] R.L. Kendall, G. Wang, K.A. Thomas, Identification of a natural soluble form of the vascular endothelial growth factor receptor, FLT-1, and its heterodimerization with KDR, Biochem. Biophys. Res. Commun. 226 (2) (1996) 324–328.
[29] H. Chen, U. Ikeda, M. Shimpo, Y. Maeda, M. Shibuya, K. Ozawa, K. Shimada, Inhibition of vascular endothelial growth factor activity by transfection with the soluble FLT-1 gene, J. Cardiovasc. Pharmacol. 36 (4) (2000) 498–502.
[30] M. Malecki, H. Trembacz, B. Szaniawska, M. Przybyszewska, P. Janik, Vascular endothelial growth factor and soluble FLT-1 receptor interactions and biological implications, Oncol. Rep. 14 (6) (2005) 1565–1569.
[31] C. Ye, C. Feng, S. Wang, K.Z. Wang, N. Huang, X. Liu, Y. Lin, M. Li, sFlt-1 gene therapy of follicular thyroid carcinoma, Endocrinology 145 (2) (2004) 817–822.
[32] Y. Hasumi, H. Mizukami, M. Urabe, T. Kohno, K. Takeuchi, A. Kume, M. Momoeda, H. Yoshikawa, T. Tsuruo, M. Shibuya, Y. Taketani, K. Ozawa, Soluble FLT-1 expression suppresses carcinomatous ascites in nude mice bearing ovarian cancer, Cancer Res. 62 (7) (2002) 2019–2023.
[33] G. Mahendra, S. Kumar, T. Isayeva, P.J. Mahasreshti, D.T. Curiel, C.R. Stockardt, W.E. Grizzle, V. Alapati, R. Singh, G.P. Siegal, S. Meleth, S. Ponnazhagan, Antiangiogenic cancer gene therapy by adeno-associated virus 2-mediated stable expression of the soluble FMS-like tyrosine kinase-1 receptor, Cancer Gene Ther. 12 (1) (2005) 26–34.
[34] Y. Takei, H. Mizukami, Y. Saga, I. Yoshimura, Y. Hasumi, T. Takayama, T. Kohno, T. Matsushita, T. Okada, A. Kume, M. Suzuki, K. Ozawa, Suppression of ovarian cancer by muscle-mediated expression of soluble VEGFR-1/Flt-1 using adeno-associated virus serotype 1-derived vector, Int. J. Cancer 120 (2) (2007) 278–284.
[35] S. Kommareddy, M. Amiji, Antiangiogenic gene therapy with systemically administered sFlt-1 plasmid DNA in engineered gelatin-based nanovectors, Cancer Gene Ther. 14 (5) (2007) 488–498.
[36] M.R. Kano, Y. Komuta, C. Iwata, M. Oka, Y.T. Shirai, Y. Morishita, Y. Ouchi, K. Kataoka, K. Miyazono, Comparison of the effects of the kinase inhibitors imatinib, sorafenib, and transforming growth factor-beta receptor inhibitor on extravasation of nanoparticles from neovasculature, Cancer Sci. 100 (1) (2009) 173–180.
[37] A. Harada, K. Kataoka, Formation of polyion complex micelles in an aqueous milieu from a pair of oppositely charged block copolymers with poly(ethylene glycol) segments, Macromolecules 28 (1995) 294–299.

[38] P.K. Dubey, V. Mishra, S. Jain, S. Mahor, S.P. Vyas, Liposomes modified with cyclic RGD peptide for tumor targeting, J. Drug Target. 12 (5) (2004) 257–264.
[39] A.J. Schraa, R.J. Kok, H.E. Moorlag, E.J. Bos, J.H. Proost, D.K. Meijer, L.F. de Leij, G. Molema, Targeting of RGD-modified proteins to tumor vasculature: a pharmacokinetic and cellular distribution study, Int. J. Cancer 102 (5) (2002) 469–475.
[40] R.M. Schiffelers, G.A. Koning, T.L. ten Hagen, M.H. Fens, A.J. Schraa, A.P. Janssen, R.J. Kok, G. Molema, G. Storm, Anti-tumor efficacy of tumor vasculature-targeted liposomal doxorubicin, J. Control. Release 91 (1–2) (2003) 115–122.
[41] A. Mitra, J. Mulholland, A. Nan, E. McNeill, H. Ghandehari, B.R. Line, Targeting tumor angiogenic vasculature using polymer-RGD conjugates, J. Control. Release 102 (1) (2005) 191–201.
[42] D.C. Bibby, J.E. Talmadge, M.K. Dalal, S.G. Kurz, K.M. Chytil, S.E. Barry, D.G. Shand, M. Steiert, Pharmacokinetics and biodistribution of RGD-targeted doxorubicin-loaded nanoparticles in tumor-bearing mice, Int. J. Pharm. 293 (1–2) (2005) 281–290.

Biomaterials 32 (2011) 3106–3114

Contents lists available at ScienceDirect

Biomaterials

journal homepage: www.elsevier.com/locate/biomaterials

Enhanced endosomal escape of siRNA-incorporating hybrid nanoparticles from calcium phosphate and PEG-block charge-conversional polymer for efficient gene knockdown with negligible cytotoxicity

Frederico Pittella [a], Mingzhen Zhang [b,d], Yan Lee [b,e], Hyun J. Kim [b], Theofilus Tockary [b], Kensuke Osada [b], Takehiko Ishii [a], Kanjiro Miyata [c], Nobuhiro Nishiyama [c], Kazunori Kataoka [a,b,c,*]

[a] Department of Bioengineering, Graduate School of Engineering, The University of Tokyo, 7-3-1 Hongo, Bunkyo-ku, Tokyo 113-8656, Japan
[b] Department of Materials Engineering, Graduate School of Engineering, The University of Tokyo, 7-3-1 Hongo, Bunkyo-ku, Tokyo 113-8656, Japan
[c] Center for Disease Biology and Integrative Medicine, Graduate School of Medicine, The University of Tokyo, 7-3-1 Hongo, Bunkyo-ku, Tokyo 113-0033, Japan
[d] School of Ophthalmology and Optometry, Wenzhou Medical College, Wenzhou, Zhejiang 325027, PR China
[e] Department of Chemistry, College of Natural Science, Seoul National University, Seoul 151-747, Republic of Korea

ARTICLE INFO

Article history:
Received 4 December 2010
Accepted 31 December 2010
Available online 26 January 2011

Keywords:
Calcium phosphate nanoparticles
Endosomal escape
Vascular endothelial growth factor (VEGF)
siRNA
Charge-conversional polymer (CCP)
Poly(ethylene glycol) (PEG)

ABSTRACT

Development of safe and efficient short interfering RNA (siRNA) delivery system for RNA interference (RNAi)-based therapeutics is a current critical challenge in drug delivery field. The major barriers in siRNA delivery into the target cytoplasm are the fragility of siRNA in the body, the inefficient cellular uptake, and the acidic endosomal entrapment. To overcome these barriers, this study is presenting a hybrid nanocarrier system composed of calcium phosphate comprising the block copolymer of poly(ethylene glycol) (PEG) and charge-conversional polymer (CCP) as a siRNA vehicle. In these nanoparticles, the calcium phosphate forms a stable core to incorporate polyanions, siRNA and PEG–CCP. The synthesized PEG–CCP is a non-toxic endosomal escaping unit, which induces endosomal membrane destabilization by the produced polycation through degradation of the flanking *cis*-aconitylamide of CCP in acidic endosomes. The nanoparticles prepared by mixing of each component was confirmed to possess excellent siRNA-loading efficiency (~80% of dose), and to present relatively homogenous spherical shape with small size. With negligible cytotoxicity, the nanoparticles efficiently induced vascular endothelial growth factor (VEGF) mRNA knockdown (~80%) in pancreatic cancer cells (PanC-1). Confocal laser scanning microscopic observation revealed rapid endosomal escape of siRNA with the nanoparticles for the excellent mRNA knockdown. The results obtained demonstrate our hybrid nanoparticle as a promising candidate to develop siRNA therapy.

1. Introduction

Since the finding of RNA interference (RNAi) in 1998 [1], the scientific community has experienced the excitement to develop a new research field. Short interfering RNA (siRNA), which allows the cleavage of the complementary mRNA for the reduced protein production in mammalian cells, provided new perspectives for potential treatment of intractable and genetic related diseases [2]. With the decoding of the human genome [3–5], it has become possible to aim a great variety of genes involved in key pathways of physiopathologies. However, a safe and efficient delivery of siRNA into the target cytoplasm has still been a major challenge. Naked siRNAs are susceptible to enzymatic degradation in the body and also possess large size (~13 kDa) and anionic charges suppressing the penetration into cellular membrane [6], thus requiring carrier systems to overcome these barriers.

Calcium phosphate (CaP) precipitates were used as transfection reagents of viral DNA for the first time in early 1970s [7], as they are believed to be non-toxic based on homology to natural inorganic materials such as teeth and bones. Notably, CaP precipitates can bind and encapsulate polyanions/nucleic acids by an easy and inexpensive method to protect the nucleic acids from enzymatic degradation and to deliver into cells. However, one of their major limitations is the uncontrollable rapid growth of calcium phosphate crystal after preparation, resulting in the formation of large agglomerates (>μm) to appreciably reduce the transfection efficiency [8–10]. In this regard, our previous studies have addressed poly(ethylene glycol) (PEG)-coating of CaP precipitates utilizing PEG-polyanion block copolymers [9,11–14]. Hydrophilic and neutral PEG is widely known

* Corresponding author. Department of Bioengineering, Graduate School of Engineering, The University of Tokyo, 7-3-1 Hongo, Bunkyo-ku, Tokyo 113-8656, Japan.
E-mail address: kataoka@bmw.t.u-tokyo.ac.jp (K. Kataoka).

0142-9612/$ – see front matter © 2011 Elsevier Ltd. All rights reserved.
doi:10.1016/j.biomaterials.2010.12.057

to provide a nanoparticle with excellent colloidal stability as well as reduced protein adsorption and immunogenicity [15–17]. Indeed, the integration of PEG-block polyanions, such as poly(aspartic acid) (PAsp) [9,12], poly(methacryl acid) [13], and siRNA [14], into CaP precipitates led to the formation of size-controllable hybrid nanoparticles with PEG palisade, which appreciably facilitated the internalization of nucleic acids by cells.

Herein, we considered the next challenge in the CaP carriers as the endosomal escape, since they are usually internalized by cells though endocytosis pathway to be delivered into acidic endosome or lysosome, resulting in enzymatic degradation of the payload nucleic acids [18]. Toward the endosomal escape with polymeric materials, our previous studies have reported a cationic polyaspartamide with a 1,2-diaminoethane side chain (poly{*N*-[*N*′-(2-aminoethyl)-2-aminoethyl] aspartamide}, PAsp(DET)) to exert strong membrane destabilization selectively in acidic endosomal compartments for efficient endosomal escape with low cytotoxicity [19–22]. Note that PAsp(DET) possesses two unique advantages for its excellent transfection: 1) the pH-selective membrane destabilization based on the distinctive two step protonation behavior in the side chain, i.e., mono-protonated form with minimal membrane damages at neutral pH and di-protonated form exerting strong membrane disruption at acidic pH [20]; 2) the spontaneous biodegradability based on the selective backbone cleavage even under physiological conditions [21].

In this work, in order to improve the endosomal escape as well as the colloidal stability of CaP precipitates, a block copolymer of PEG and an endosomal escaping polymer was synthesized and integrated into the CaP nanoparticles incorporating siRNA. Indeed, we modified the flanking primary amines of PEG-PAsp(DET) with *cis*-aconitic anhydride [23,24] to convert the cationic charges to net negative ones with two carboxylates of the *cis*-aconityl moiety (PEG-poly{*N*-[*N*′-(*N*″-*cis*-aconityl-2-aminoethyl)-2-aminoethyl]aspartamide}, PEG-PAsp(DET-Aco)) for effective binding to CaP nanoparticles. Noteworthy, the prepared *cis*-aconitylamide shows high stability at neutral and basic pHs but it becomes cleavable at acidic pH to reproduce cationic PAsp(DET) from anionic PAsp(DET-Aco) in endosome/lysosome, which is termed the charge-conversional polymer [23–25]. The hybrid nanoparticle prepared from PEG-PAsp (DET-Aco), siRNA, and CaP does not contain inherent toxic materials, such as polycations, thereby leading to potentially lower toxicity compared to conventional polyplex carriers from polycations and siRNA. Thus, the nanoparticles prepared by simple mixing of each component were physicochemically and biologically characterized by the comparison with non-charge-conversional control polyanions to demonstrate the utility of our hybrid system from the PEG–charge-conversional polymer for siRNA delivery.

2. Material and methods

2.1. Materials

cis-Aconitic anhydride, tricarballylic acid, and Dulbecco's modified eagle's medium (DMEM) were purchased from Sigma–Aldrich (St. Louis, MO). α-Methoxy-ω-amino-poly(ethylene glycol) (MeO–PEG–NH_2) (M_w: 12,000) and β-benzyl-L-aspartate *N*-carboxyanhydride (BLA–NCA) were obtained from NOF Co, Inc. (Tokyo, Japan) and Chuo Kaseihin Co., Inc. (Tokyo, Japan), respectively. *N*-Methyl-2-pyrrolidone (NMP), diethylenetriamine (DET), dimethyl sulfoxide (DMSO), *N*,*N*-dimethylformamide (DMF), dichloromethane (DCM), and acetic anhydride were purchased from Tokyo Chemical Industry Co. Ltd. (Tokyo, Japan) or Nacalai Tesque (Tokyo, Japan), and used after a conventional distillation. Acetic acid, acetonitrile, acetone, diethyl ether, and hydrochloric acid were purchased from Wako Pure Chemical Industries Ltd. (Osaka, Japan). Fetal bovine serum (FBS) was purchased from Dainippon Sumitomo Pharma Co., Ltd. (Osaka, Japan). The primers for human actin and human VEGF were synthesized by Hokkaido System Science (Hokkaido, Japan) and the sequences are: CCAACCGCGAGAAGATGA (actin forward); CCAGAGGCGTACAGGGATAG (actin reverse); AGTGGTCCCAGGCTGCAC (VEGF forward); TCCATGAACTTCACCACTTCGT (VEGF reverse). All the siRNAs were synthesized by Hokkaido System Science (Hokkaido, Japan) and the sequences of VEGF siRNA (siVEGF) are: 5′-GGAGUACCCUGAUGAGAUCdTdT-3′ (sense); 5′-GAUCUCAUCAGGGUACUCCdTdT-3′ (antisense), and GL3 luciferase siRNA (siGL3) are: 5′-CUU ACG CUG AGU ACU UCG AdTdT-3′ (sense); 5′-UCG AAG UAC UCA GCG UAA GdTdT-3′ (antisense).

2.2. Synthesis of block copolymer with poly(ethylene glycol) and charge-conversional polymer (PEG–CCP) segments

2.2.1. Synthesis of poly(ethylene glycol)-b-poly{*N*-[*N*-(2-aminoethyl)-2-aminoethyl] aspartamide} (PEG-PAsp(DET))

PEG-PAsp(DET) was prepared as previously reported with slight modification [21]. Briefly, BLA–NCA (780 mg; 3.13 mmol) was dissolved in 0.7 mL of DMF, and then in 7.3 mL of DCM. The polymerization was initiated from the primary amino group of MeO–PEG–NH_2 (M_w = 12,000, 500 mg; 0.0417 mmol) to obtain PEG–PBLA (1100 mg) as a precursor. Size exclusion chromatography (SEC) was performed to determine the molecular weight distribution (M_w/M_n) of the obtained PEG–PBLA using a TOSOH HLC-8220 equipped with TSK gel columns (SuperAW4000 and SuperAW3000 × 2; eluent: NMP with 50 mM LiBr; flow rate: 0.3 mL min^{-1}; temperature: 40 °C) and an internal refractive index (RI) detector. The M_w/M_n was confirmed to be 1.07 from the SEC chart using PEG standards for the M_w calibration (data not shown). The degree of polymerization of PBLA in PEG–PBLA was determined to be 96 from the peak intensity ratio of the methylene protons of PEG (–OCH_2CH_2–, δ = 3.5 ppm) to the benzyl protons of PBLA ($C_6H_5CH_2$–, δ = 5.1 and 7.3 ppm) in the ^1H NMR measurement (data not shown). All of the NMR assays were performed using (3-(trimethylsilyl)-3,3,2,2-tetradeuteropropionic acid sodium salt d_4-TSPA) as an internal standard. Then, PEG–PBLA (1100 mg) was dissolved in NMP (2 mL) and cooled at 5 °C. Diethylenetriamine (DET) (3 mL; 100 equiv to benzyl groups of PBLA segment) was diluted with the same volume of NMP, and then the first solution was added and stirred for 4 h at 0 °C (ice bath). The reaction was stopped adding the polymer solution to cold 20% acetic acid (30 mL) drop-by-drop. The neutralized solution was dialyzed against 0.01 M hydrochloric acid solution and then in de-ionized water at 4 °C. As a hydrochloride salt form, a white powder was obtained after lyophilization of the dialyzed solution (91.2 mg, 69.6% yield). The quantitative conversion of the BLA to Asp(DET) was confirmed from the peak intensity ratio of the methylene protons in PEG (–OCH_2CH_2–, δ = 3.7 ppm) to the ethylene protons in the 1,2-diaminoethane moiety ($H_2N(CH_2)_2NH(CH_2)_2NH$–, δ = 2.8–3.4 ppm) in the ^1H NMR spectrum in D_2O at 50 °C (Supporting Information).

2.2.2. Synthesis of poly(ethylene glycol)-b-poly{*N*-[*N*′-(*N*″-*cis*-aconityl-2-aminoethyl)-2-aminoethyl]aspartamide} (PEG-PAsp(DET-Aco))

PEG-PAsp(DET) (17.5 mg, 0.0538 mmol of primary amine) was dissolved in 0.5 M $NaHCO_3$ at pH 9.1 (50 mL). *cis*-Aconitic anhydride powder (420 mg, 2.69 mmol) was added to the solution slowly and stirred at 0 °C for 2 h. The reaction mixture was purified by centrifugal ultrafiltration with Amicon Ultra (MWCO = 10,000; Millipore (Billerica, MA)) three times with de-ionized water at 4 °C. The final product was obtained as a white powder after lyophilization (14.9 mg, 64.7% yield). The quantitative conversion of primary amines in Asp(DET) side chain to *cis*-aconitylamide was confirmed from the peak intensity ratio of the methine protons in the main chain (–$COCH_2CH$(CO–)NH–, –$COCH(CH_2$–)NH–, δ = 4.8 ppm) to methine protons of the *cis*-aconityl moiety (–COCH:C(COONa)CH_2COONa, δ = 6.0 ppm) in ^1H NMR spectrum in D_2O at 50 °C (Fig. 1).

2.3. Synthesis of block copolymer with poly(ethylene glycol) and non-charge-conversional polymers (PEG–nCCP) segments

2.3.1. Synthesis of carballylic anhydride

Carballylic anhydride was prepared as previously reported [26] with slight modification. Briefly, tricarballylic acid (4.4 g, 0.025 mol) was reacted with acetic anhydride (4.73 mL, 0.05 mol) at 45 °C for 1 h. The excess of acetic anhydride was evaporated under reduced pressure. Further, the product was dissolved in the minimum amount of ethyl acetate at 80 °C and filtered. The solution was allowed to stand for 5 h at room temperature and then overnight at 4 °C. The obtained crystal was then vacuum-filtered, washed with excess of diethyl ether, and then dried in vacuum to yield a white crystal (760 mg, 19.2% yield). The reaction was confirmed by ^1H NMR spectrum in acetone at 25 °C (–$COCH_2CH(CH_2COOH)CO$–, δ = 2.94, 2.86 ppm), (CH_2COOH, δ = 2.44 ppm) (data not shown).

2.3.2. Synthesis of poly(ethylene glycol)-b-poly{*N*-[*N*′-(*N*″-carballylyl-2-aminoethyl)-2-aminoethyl]aspartamide} (PEG-PAsp(DET-Car))

PEG-PAsp(DET) (15 mg, 0.046 mmol of primary amine) was dissolved in 0.5 M $NaHCO_3$ at pH 9.1 (50 mL). Carballylic anhydride powder (Car) (363 mg, 2.3 mmol) was added to the solution slowly and stirred at 0 °C for 2 h. The reaction mixture was purified by centrifugal ultrafiltration with Amicon Ultra (MWCO = 10,000; Millipore (Billerica, MA)) three times with de-ionized water at 4 °C. The final product was obtained as a white powder after lyophilization (13.5 mg, 68.3% yield). The quantitative conversion of the primary amines in the Asp(DET) side chain to carballylylamide was confirmed from the peak intensity ratio of the methine protons in the main chain (–$COCH_2CH$(CO–)NH–, –$COCH(CH_2$–)NH–, δ = 4.8 ppm) to the methylene protons of the carballylyl moiety (–CH_2CH(COONa)CH_2COONa, δ = 2.5) in the ^1H NMR spectrum in D_2O at 50 °C (Supporting Information).

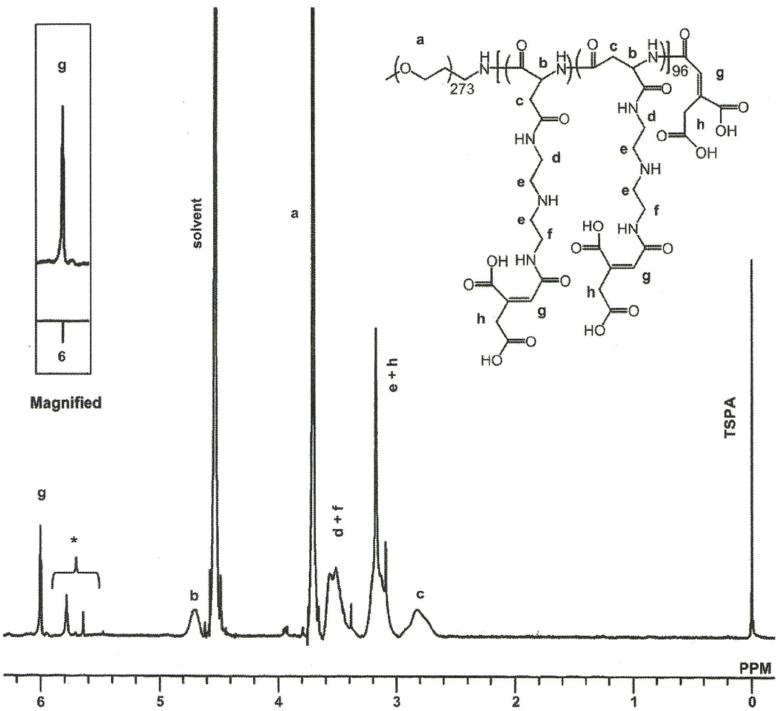

Fig. 1. ^{1}H NMR spectrum of the synthesized PEG-polyanion block copolymer, PEG-PAsp(DET-Aco) (Concentration: 10 mg/mL, Solvent: D_2O, Temperature: 50 °C). *Decarboxilated itaconitylamide (Supporting Information).

2.3.3. Synthesis of poly(ethylene glycol)-b-poly(aspartic acid) (PEG-PAsp)

PEG–PBLA (20 mg, 0.06 mmol) was dissolved in acetonitrile (1.5 mL). Aqueous sodium hydroxide (0.5 N, 6 mL, 50 equiv to benzyl group of PBLA segment) was added to the first solution and allowed to react for 1 h stirring at room temperature. The solution was dialyzed against de-ionized water. A white powder was obtained after lyophilization of the dialyzed solution (18.2 mg, 93.0% yield). The complete deprotection of the flanking benzyl esters in PBLA was confirmed by the peak disappearance of benzyl protons of PBLA ($-CH_2C_6H_5$, $\delta = 7.3$) in the ^{1}H NMR spectrum in D_2O at 50 °C (data not shown).

2.4. Preparation of PEG-polyanion/siRNA/CaP hybrid nanoparticles

A solution of 2.5 M $CaCl_2$ was diluted in 10 mM Tris/HCl buffer (pH 7.5) (1 μL: 11.5 μL). Another solution containing PEG-PAsp(DET-Aco) or PEG-PAsp(DET-Car) (1000 μg/mL) in 10 mM Tris/HCl buffer (pH 7.5) was mixed with a solution of 15 μM siRNA in 10 mM Hepes buffer (pH 7.2) and with 50 mM Hepes buffer containing 1.5 mM Na_3PO_4 and 140 mM NaCl (pH 7.5) (2.5 μL: 5 μL: 5 μL). The former solution was mixed with the latter solution by pipetting for around 20 s (final siRNA concentration; 3 μM). A control nanoparticle containing PEG-PAsp was built as previously described [9]. Each sample solution was used immediately after preparation.

2.5. Dynamic light scattering (DLS)

For the determination of size distribution of hybrid nanoparticles, DLS measurements were carried out at 25 °C using a Zetasizer Nano ZS (Malvern Instruments, UK) at a detection angle of 173° with a He–Ne laser (633 nm) as the incident beam. The data obtained from the rate of decay in the photon correlation function were analyzed with a cumulant method to obtain the corresponding hydrodynamic diameters and polydispersity indices (PdI) (μ/Γ^2) of the nanoparticles.

2.6. Determination of siRNA encapsulated in hybrid nanoparticle

The assay to estimate the amount of siRNA encapsulated in hybrid nanoparticles was carried out as previously reported [11]. Briefly, the sample solutions were centrifuged at 15,000g for 30 min to precipitate the nanoparticles. The supernatant was carefully collected to determine the siRNA concentration by measurement of absorbance at 260 nm (Abs_{260}). The percentage of the loaded siRNA was calculated as follows;

Encapsulated percentage (%) = 100 − (Abs_{260} after centrifuge)/(Abs_{260} before centrifuge) × 100

2.7. Transmission electron microscopy (TEM) observation

TEM observation was conducted using H-7000 electron microscope (Hitachi, Tokyo, Japan) operated at 75 kV acceleration voltages. Copper TEM grids with carbon-coated collodion film were glow-discharged for 20 s using an Eiko IB-3 ion coater (Eiko Engineering Co. Ltd., Japan). The grids were dipped into complex solution with 3 μM siRNA, which was mixed with uranyl acetate solution (2% (w/v)), for 30 s. After excess solution was removed using a filter paper, the sample grids were allowed to dry in air and then TEM observation was carried out.

2.8. Cell viability assay

For the cytotoxicity assay, PanC-1 cells (Pancreatic cancer cells, ATCC Number: CRL-1469) were seeded with 100 μL of DMEM containing 10% FBS in a 96 well plate (5000 cells/well) and incubated for 24 h. The nanoparticles (containing 10–1500 nM siRNA) were added with the fresh medium containing 10% FBS, and the cell viability was evaluated after 48-h incubation by Cell Counting Kit-8 (Dojindo, Kumamoto, Japan) according to the protocol provided by the manufacturer. Each well was measured by reading the absorbance at 450 nm in a Microplate Reader (Bio-Rad Model 680, Bio-Rad Laboratories, UK). The results were expressed as the percentage (%) of the control cells, which were incubated only with the culture medium.

2.9. Confocal laser scanning microscopy (CLSM) observation

PanC-1 cells were cultured with 1.5 mL of DMEM containing 10% FBS on 35-mm glass-base dishes (Iwaki, Japan) at 5×10^4 cells/dish. After 24 h, the medium was exchanged with fresh one and Cy5-labeled siRNA-containing nanoparticles were applied to the dish (100 nM siRNA). The nuclei and the endosome/lysosome were stained with Hoechst 33342 (Dojindo Laboratories, Kumamoto, Japan) for 5 min and LysoTracker Green (Molecular Probes, Eugene, OR) for 15 min before CLSM imaging, respectively. Cells were rinsed 3 times with PBS and fresh medium was added prior to the imaging. CLSM images were acquired at 3 and 24 h after nanoparticle administration, using a Zeiss LSM 510 META (Carl Zeiss, Germany) with a water-immersion 63× objective (C-Apochromat, Carl Zeiss). Excitation wavelengths were 488 nm (argon laser), 633 nm (He–Ne laser), and 710 nm (Mai Tai laser, operated in a two-photon mode) for LysoTracker, Cy5, and Hoechst 33342, respectively. The co-localization ratio was calculated as previously described [24] with the formula:

Co-localization ratio = number of yellow pixels/number of yellow and red pixels.

2.10. Real-time reverse transcription (RT)-PCR

PanC-1 cells were seeded with 2000 μL of DMEM containing 10% FBS on a 6 well plate at 8×10^4 cells/well. After 24 h, nanoparticles were added with fresh medium (60 nM siRNA). After 3 h of exposing the cells to nanoparticles, the medium was changed to fresh one. Twenty four hours later, cells were harvested and RNA was extracted using the RNeasy Mini Kit (Qiagen, Valencia, CA), according to the manufacturer's instruction. The amount of extracted RNA was measured and standardized after the genomic DNA elimination for the cDNA synthesis (QuantiTect Reverse Transcription, Quiagen, Valencia, CA). Real-time RT-PCR was performed using the ABI 7500 Fast Real-time RT-PCR System (Applied Biosystems, Foster City, CA) and QuantiTect SYBR Green PCR Master Mix (Qiagen, Valencia, CA). The actin was used as a house-keeper gene and the obtained data were normalized before statistical analysis.

2.11. Statistical analysis

The analysis of variance (ANOVA) was performed to test the treatment effects, and Bonferroni's test was used as *post hoc* pairwise comparisons between individual treatment groups, using the software GraphPad Prisma 3.0 (GraphPad Software, Inc.). Statistical significance is represented as * for $p < 0.05$ and ** for $p < 0.01$. Unless indicated, all experiments were performed in triplicate ($N = 3$) and the results reported were expressed as mean values (±SEM).

3. Results and discussion

3.1. Synthesis of charge-conversional and non-charge-conversional polymers

The synthesis route of PEG–PAsp(DET-Aco) as a charge-conversional polyanion is illustrated in Scheme 1, as well as two polyanions used as controls without the charge-conversional property. PEG–PAsp(DET) was synthesized from PEG–PBLA (M_w of PEG 12,000; DP of PBLA 96) by aminolysis reaction with excess of DET molecules. The ^{1}H NMR measurement revealed the quantitative introduction of the *N*-(2-aminoethyl)-2-aminoethyl moiety for successful synthesis of PEG–PAsp(DET) (data not shown). Further, the *cis*-acontyl moiety (Aco) was introduced into the primary amine in the side chain of PAsp(DET) by reacting *cis*-aconitic anhydride with PEG–PAsp(DET) to form an acid-labile *cis*-aconitylamide in the side chain. The quantitative conversion of primary

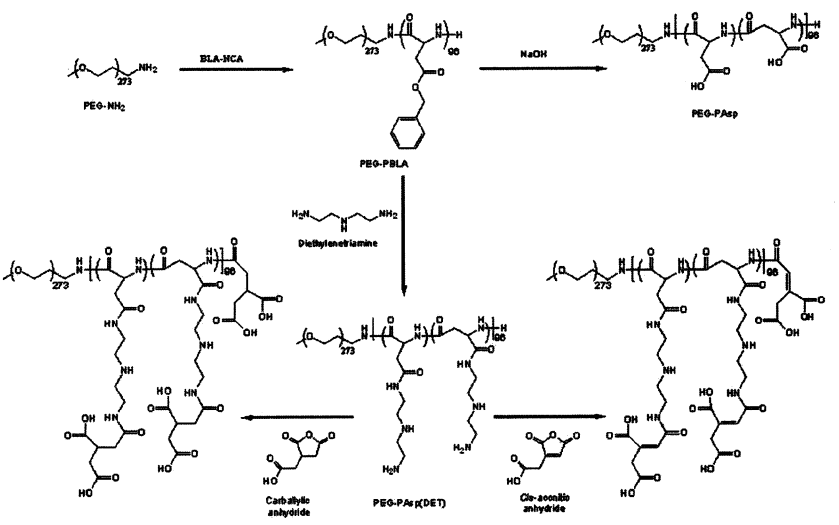

Scheme 1. Synthetic routes of PEG–PAsp(DET-Aco), PEG–PAsp(DET-Car), and PEG–PAsp.

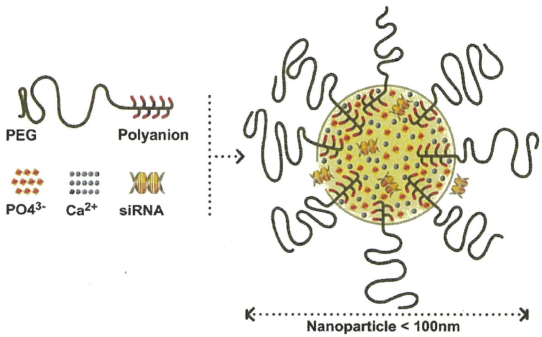

Fig. 2. Schematic illustration of PEG-polyanion/siRNA/CaP hybrid nanoparticles.

amines in Asp(DET) side chain to *cis*-aconitylamide was confirmed from the peak intensity ratio of the methine protons in the main chain to methine protons of the *cis*-aconityl moiety in the ^{1}H NMR spectrum in D_2O (Fig. 1). Although it was also possible to observe the formation of reaction subproducts [27], the desired product of PEG-PAsp(DET-Aco) was obtained in a high ratio (80%). PEG-PAsp (DET-Car) without the acid-labile bond as a control was synthesized by reacting PEG-PAsp(DET) with carballylic anhydride similarly. The quantitative conversion of the primary amines in the Asp(DET) side chain to carballylylamide was confirmed from the peak intensity ratio of the methine protons in the main chain to the methine and methylene protons of carballylyl moiety in the ^{1}H NMR spectrum in D_2O (Supporting Information). In addition, another control polyanion, PEG-PAsp, was prepared by the deprotection of benzyl ester group from PEG–PBLA. The successful deprotection of benzyl ester group was confirmed from the corresponding peak disappearance in the ^{1}H NMR spectrum in D_2O (data not shown). Note that all the reactions were confirmed to proceed without the spontaneous main-chain cleavage [21] from aqueous GPC charts of obtained polymers (data not shown).

3.2. PEG-polyanion/siRNA/CaP hybrid nanoparticle formation and characterization

Great advantages in the utilization of CaP precipitates as a transfection reagent are the fact that they are prepared by a simple and inexpensive method, and also that it efficiently binds/encapsulates polyanions/nucleic acids during the formation process [28,29]. Through self-assembly, CaP nanoparticles containing nucleic acid are formed by the precipitation method in which calcium chloride and phosphate solutions are mixed in the presence of siRNA. However, simple CaP precipitates have potential problems to overcome for efficient nucleic acids delivery; one is the increase in size with time to form large agglomerates in aqueous solutions, and another is poor endosomal escape. To prevent the size increase in CaP precipitates, our previous studies have addressed a preparation of PEG-coated CaP hybrid nanoparticles by mixing of PEG-polyanion block copolymers [9,11–14]. In this study, for further improvement of the PEG-coated CaP nanoparticles, we focused on endosomal escape of the nanoparticles to enhance the gene knockdown efficiency, thus applying a charge-conversional structure PAsp(DET-Aco) [23,24] for the polyanionic segment. Indeed, the hybrid nanoparticles were prepared from the inorganic CaP core, siRNA as a therapeutic payload, and the PEG-PAsp(DET-Aco) as a charge-conversional unit for endosomal escape with minimal cytotoxicity, by mixing calcium and phosphate ionic solutions containing siRNA and the charge-conversional polymer as illustrated in Fig. 2.

The TEM observations with uranyl acetate as a staining agent (Fig. 3A) revealed hybrid nanoparticles with relatively homogenous spherical shape and average size of 42 ± 5 nm. Furthermore, the DLS measurements provided a size histogram in number statistics showing a narrow unimodal distribution with the peak at 38 nm

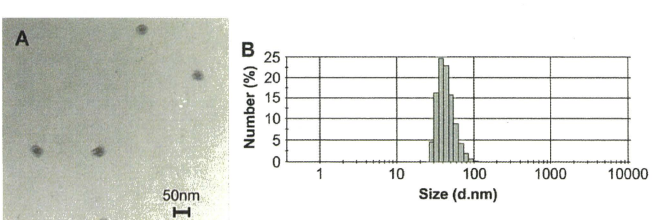

Fig. 3. Size and morphology of PEG-PAsp(DET-Aco)/siRNA/CaP hybrid nanoparticles. A: TEM image (Scale Bar: 50 nm). B: Histogram in number statistics determined by DLS measurement (1 mg/mL PEG-PAsp(DET-Aco) and 3 μM siRNA).

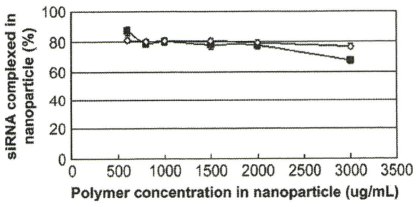

Fig. 4. Percentage of siRNA loaded by the hybrid nanoparticle at varying polymer concentrations (3 μM siRNA). Closed square: PEG-PAsp(DET-Aco), Open diamond: PEG-PAsp(DET-Car).

(Fig. 3B), which was well correlated to the size determined by the TEM observations (Fig. 3A). Samples were confirmed to have the same size even after prolonged incubation time. These results indicate that hybrid nanoparticles can be obtained in a controllable manner using the charge-conversional polymer as colloidal stability agent.

The amount of siRNA encapsulated in the hybrid nanoparticles was monitored against polyanion concentration, determined by the centrifugal assay as previously reported [11]. Effective encapsulation of siRNA in the nanoparticles (around 80%) was confirmed in PEG-PAsp(DET-Aco) concentration between 600 and 2000 μg/mL, while a slight decrease was observed at the concentration of 3000 μg/mL (around 70%) (Fig. 4). Note that the similar binding tendency was observed for the nanoparticle from PEG-PAsp(DET-Car). The siRNA-loading capacities obtained here were close to those found in our previous work with PEG-PAsp (around 85%) [11], indicating efficient entrapment of siRNA by this method regardless of polyanion structures.

3.3. Gene knockdown and cell viability assays

The development of an effective and non-cytotoxic carrier is the main challenge to the success in RNAi therapy. We verified the gene knockdown efficiency of the hybrid nanoparticles to a cultured pancreatic cancer cell (PanC-1) by measuring the level of mRNA. Here, vascular endothelial growth factor (VEGF) was chosen as a target gene because many cancer cells up-regulate VEGF expression to promote angiogenesis, a process characterized by the formation of new blood vessels from a pre-existing vascular network [30,31], facilitating the tumor growth and proliferation. Hence, VEGF knockdown in such cancer cells with siRNA *in vivo* is expected to be a promising strategy to suppress the tumor growth and control cancer evolution (anti-angiogenic therapy).

Hybrid nanoparticles containing 60 nM siVEGF or siLuc as a non-targeted control sequence were applied to PanC-1 cells, and after 3 h of exposure time the medium was replaced and cells were further incubated for 24 h. Thereafter, the real-time RT-PCR analysis was used to determine the mRNA for VEGF. The results revealed that all the tested hybrid nanoparticles with siVEGF possessed potential gene knockdown activity, whereas the nanoparticles with siLuc and naked siVEGF showed no gene knockdown (Fig. 5), indicating the siVEGF sequence-specific gene knockdown with the hybrid nanoparticles. Among them, the nanoparticle from PEG-PAsp(DET-Aco) presented the only significant and highest gene knockdown (~82%). The comparison of PEG-PAsp(DET-Aco) with the other PEG-polyanions strongly suggests that the acid-labile *cis*-aconitylamide in PEG-PAsp(DET-Aco) should be essential for the significant gene knockdown. Next, the cytotoxicity of the hybrid nanoparticles was evaluated to PanC-1 cells. A wide range of siRNA concentration was tested from 10 to 1500 nM along with the increase in all the other components. As shown in Fig. 6, no significant cytotoxicity was observed for both hybrid nanoparticles from PEG-PAsp(DET-Aco/Car) even at the highest concentration (50 μg/mL PEG-polyanion, 1.5 μM siRNA). From these results, we concluded that the hybrid nanoparticles from PEG-PAsp(DET-Aco) allowed efficient siRNA delivery into the cytoplasm of cultured PanC-1 with negligible cytotoxicity.

3.4. Cellular uptake and intracellular trafficking

In siRNA transfection process, after cellular internalization as the first hurdle, siRNA carriers will be delivered to early endosomes,

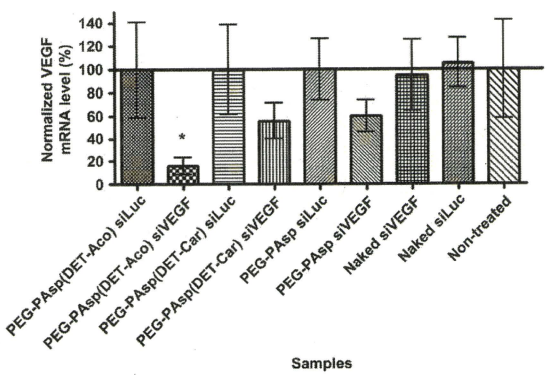

Fig. 5. Gene knockdown in PanC-1 at 24 h after 3 h of nanoparticles exposition to cells (60 nM siRNA, $N = 9$). Controls were set as 100%. *$p < 0.05$ comparing to controls (ANOVA followed by Bonferroni).

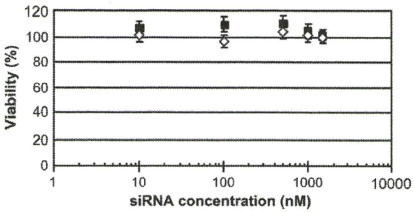

Fig. 6. Cell viability of PanC-1 cells incubated with hybrid nanoparticles for 48 h ($N = 6$). siLuc concentration was changed from 10 to 1500 nM, corresponding to the polymer concentration from 0.7 to 50 μg/mL. Closed square: PEG-PAsp(DET-Aco), Open diamond: PEG-PAsp(DET-Car).

followed by the movement to late endosomes/lysosomes for siRNA degradation [6]. Thus, the smooth endosomal escape is a critical requirement for the effective gene silencing with siRNA. In the preceding section, the utility of PEG-PAsp(DET-Aco) was demonstrated for significant VEGF mRNA knockdown without marked cytotoxicity. Here, we verified whether the excellent gene knockdown is attributed to endosomal escape with PEG-PAsp(DET-Aco) along with our initial hypothesis. Accordingly, we observed the intracellular trafficking of each hybrid nanoparticle after 3- and 24-h incubation with PanC-1 cells. In the obtained images, Cy5-siRNA, endosomes/lysosomes, and nuclei were shown in red, green, and blue, respectively, and thus yellow pixels result in the merge of red and green pixels, indicating the co-localization of Cy5-siRNA with endosome/lysosome. The images of PanC-1 cells treated with PEG-PAsp(DET-Aco)/PEG-PAsp(DET-Car) nanoparticles displayed red and/or yellow regions with 3-h incubation (Fig. 7A and B), indicating that both of the nanoparticles allowed the significant cellular uptake of Cy5-siRNA. In these two images, only the nanoparticles containing PEG-PAsp(DET-Aco) in the formulation presented widely extended red regions in cells (Fig. 7A), corresponding to the presence of Cy5-siRNA in the cytoplasm. In contrast, the cells treated with the other nanoparticles containing PEG-PAsp(DET-Car) mainly displayed perinuclear yellow spots (Fig. 7B), indicating the endosomal/lysosomal capture of Cy5-siRNA. These results are well consistent with our hypothesis that the integration of PEG-PAsp(DET-Aco) into the nanoparticles intensely facilitates the endosomal escape of the hybrid nanoparticles in the early stage of transfection, presumably due to the charge-conversional property

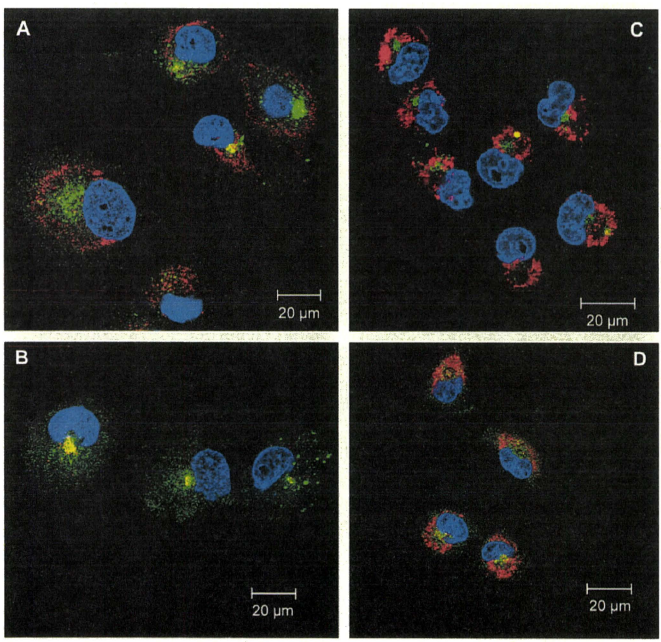

Fig. 7. Confocal laser scanning microscopic observation for intracellular trafficking of hybrid nanoparticles. Images were taken at 3 and 24 h after nanoparticle application. A: PEG-PAsp(DET-Aco), B: PEG-PAsp(DET-Car) nanoparticles incubated for 3 h (100 nM siRNA). C: PEG-PAsp(DET-Aco), D: PEG-PAsp(DET-Car) nanoparticles incubated for 24 h (100 nM siRNA). Blue: Hoechst at 710 nm (two-photon excitation); Green: Lysotracker at 488 nm; and Red: Cy5 at 633 nm.

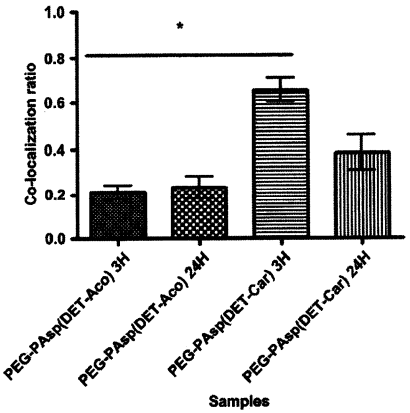

Fig. 8. Co-localization ratio of Cy5-labeled siRNA with endosome/lysosome obtained by analyzing the images. Results were expressed as mean ± SEM (from three cells) (*$p < 0.01$).

to reproduce the endosomal membrane destabilizing polycation, PAsp(DET), in the acidic endocytic vesicles. On the other hand, after 24-h incubation, the cells treated with PEG-PAsp(DET-Car) nanoparticles obviously increased red regions (Fig. 7D), suggesting that the hybrid nanoparticles might originally have an endosomal escaping ability apart from the charge-conversional polymers. A possible explanation of this delayed endosomal escape is that CaP core disassembles under a low ionic condition in endocytic vesicles for increased-ion induced-osmotic pressure to induce endosomal membrane disruption [11], similar to the proton sponge hypothesis known to polyethyleneimine [32]. Eventually, the co-localization of Cy5-siRNA with endosome/lysosome was quantitatively analyzed for PEG-PAsp(DET-Aco) and PEG-PAsp(DET-Car), as summarized in Fig. 8. The obtained tendency in endosomal escape of each nanoparticle is well correlated with the result in the gene knockdown experiment (Fig. 5). Earlier endosomal escape of siRNA by PEG-PAsp (DET-Aco) probably leads to more efficient gene knockdown with the nanoparticles.

4. Conclusion

This work was aimed to develop a hybrid nanocarrier system consisting of CaP and the PEG–charge-conversional polymer for safe and efficient siRNA delivery. To improve the endosomal escape of the nanoparticles, we integrated the charge-conversional polymer PEG-PAsp(DET-Aco) into the nanoparticles, in which PEG-PAsp (DET-Aco) induces the destabilization of endosomal membrane by producing a polycation PAsp(DET) via the selective cleavage of *cis*-aconitylamide in acidic endosome/lysosome. The size less than 100 nm with narrow size distribution and a high siRNA-loading capacity were confirmed for PEG-PAsp(DET-Aco)/siRNA/CaP nanoparticles, which achieved strong VEGF knockdown to PanC-1 with negligible cytotoxicity through the rapid endosomal escape. These findings demonstrate our hybrid system as a promising candidate to future *in vivo* siRNA applications for pancreatic cancer treatment based on anti-angiogenic therapy.

Acknowledgments

This research is supported by the Japan Society for the Promotion of Science (JSPS) through its "Funding Program for World-Leading Innovative R&D on Science and Technology (FIRST Program)". F.P. acknowledges the fellowship from Ministry of Education, Science, Sports and Culture, Japan (MEXT).

Appendix

Figures with essential color discrimination. Figs. 2, 3 and 7 in this article are difficult to interpret in black and white. The full color images can be found in the online version, at doi:10.1016/j.biomaterials.2010.12.057.

Appendix. Supporting information

Supplementary data associated with this article can be found, in the online version, at doi:10.1016/j.biomaterials.2010.12.057.

References

[1] Fire A, Xu S, Montgomery MK, Kostas SA, Driver SE, Mello CC. Potent and specific genetic interference by double-stranded RNA in *Caenorhabditis elegans*. Nature 1998;391:806–11.
[2] Elbashir SM, Harborth J, Lendeckel W, Yalcin A, Weber K, Tuschl T. Duplexes of 21-nucleotide RNAs mediate RNA interference in cultured mammalian cells. Nature 2001;411:494–8.
[3] International Human Genome Sequencing Consortium. Initial sequencing and analysis of the human genome. Nature 2001;409:860–921.
[4] Venter JC, Adams MD, Myers EW, Li PW, Mural RJ, Sutton GG, et al. The sequence of the human genome. Science 2001;291:1304–51.
[5] International Human Genome Sequencing Consortium. Finishing the euchromatic sequence of the human genome. Nature 2004;431:931–45.
[6] Whitehead KA, Langer R, Anderson DG. Knocking down barriers: advances in siRNA delivery. Nat Rev Drug Discov 2009;8(2):129–38.
[7] Graham FL, van der Eb AJ. A new technique for the assay of infectivity of human adenovirus 5 DNA. Virology 1973;52:456–67.
[8] Jordan M, Schallhorn A, Wurm FM. Transfecting mammalian cells: optimization of critical parameters affecting calcium–phosphate precipitate formation. Nucleic Acids Res 1996;24:596–601.
[9] Kakizawa Y, Kataoka K. Block copolymer self-assembly into monodispersive nanoparticles with hybrid core of antisense DNA and calcium phosphate. Langmuir 2002;18:4539–43.
[10] Maitra A. Calcium phosphate nanoparticles: second-generation nonviral vectors in gene therapy. Expert Rev Mol Diagn 2005;5(6):893–905.
[11] Kakizawa Y, Furukawa S, Kataoka K. Block copolymer-coated calcium phosphate nanoparticles sensing intracellular environment for oligodeoxynucleotide and siRNA delivery. J Control Release 2004;97:345–56.
[12] Kakizawa Y, Miyata K, Furukawa S, Kataoka K. Size-controlled formation of a calcium phosphate-based organic-inorganic hybrid vector for gene delivery using poly(ethylene glycol)-*block*-poly(aspartic acid). Adv Mater 2004;16 (8):699–702.
[13] Kakizawa Y, Furukawa S, Ishii A, Kataoka K. Organic–inorganic hybrid-nanocarrier of siRNA constructing through the self-assembly of calcium phosphate and PEG-based block aniomer. J Control Release 2006;111:368–70.
[14] Zhang MZ, Ishii A, Nishiyama N, Matsumoto S, Ishii T, Yamasaki Y, et al. PEGylated calcium phosphate nanocomposites as smart environment-sensitive carriers for siRNA delivery. Adv Mater 2009;21(34):3520–5.
[15] Francis G, Delgado C, Fisher D, Malik F, Agrawal AK. Polyethylene glycol modification: relevance to improved methodology to tumour targeting. J Drug Target 1996;3:321–40.
[16] Monfardini C, Veronese FM. Stabilization of substances in the circulation. Bioconjug Chem 1998;9:418–50.
[17] Kataoka K, Harada A, Nagasaki Y. Block copolymer micelles for drug delivery: design, characterization and biological significance. Adv Drug Deliv Rev 2001;47:113–31.
[18] Dominska M, Dykxhoorn DM. Breaking down the barriers: siRNA delivery and endosome escape. J Cell Sci 2010;123:1183–9.
[19] Kanayama N, Fukushima S, Nishiyama N, Itaka K, Jang W-D, Miyata K, et al. A PEG-based biocompatible block catiomer with high buffering capacity for the construction of polyplex micelles showing efficient gene transfer toward primary cells. ChemMedChem 2006;1:439–44.
[20] Miyata K, Oba M, Nakanishi M, Fukushima S, Yamasaki Y, Koyama H, et al. Polyplexes from poly(aspartamide) bearing 1,2-diaminoethane side chains induce pH-selective, endosomal membrane destabilization with amplified transfection and negligible cytotoxicity. J Am Chem Soc 2008;130(48): 16287–94.

[21] Itaka K, Ishii T, Hasegawa Y, Kataoka K. Biodegradable polyamino acid-based polycations as safe and effective gene carrier minimizing cumulative toxicity. Biomaterials 2010;31(13):3707–14.
[22] Kim HJ, Ishii A, Miyata K, Lee Y, Wu S, Oba M, et al. Introduction of stearoyl moieties into a biocompatible cationic polyaspartamide derivative, PAsp (DET), with endosomal escaping function for enhanced siRNA-mediated gene knockdown. J Control Release 2010;145(2):141–8.
[23] Lee Y, Miyata K, Oba M, Ishii T, Fukushima S, Han M, et al. Charge conversion ternary polyplex with endosomes disruption moiety: a technique for efficient and safe gene delivery. Angew Chem Int Ed Engl 2008;120:5241–4.
[24] Sanjoh M, Hiki S, Lee Y, Oba M, Miyata K, Ishii T, et al. pDNA/poly(l-lysine) polyplexes functionalized with a pH-sensitive charge-conversional poly (aspartamide) derivative for controlled gene delivery to human umbilical vein endothelial cells. Macromol Rapid Commun 2010;31(13):1181–6.
[25] Lee Y, Fukushima S, Bae Y, Hiki S, Ishii T, Kataoka K. A protein nanocarrier from charge-conversion polymer in response to endosomal pH. J Am Chem Soc 2007;129:5362–3.
[26] Elgazwy A-SSH. Facile synthesis of (*R*, *R*) and of (*R*, *S*) tricarballylic acid anhydride and imide derivatives. Molecules 2000;5:665–73.
[27] Dinand E, Zloh M, Brocchini S. Competitive reactions during amine addition to *cis*-aconityl anhydride. Aust J Chem 2002;55:467–74.
[28] Sokolova VV, Radtke I, Heumann R, Epple M. Effective transfection of cells with multi-shell calcium phosphate–DNA nanoparticles. Biomaterials 2006;27:3147–53.
[29] Zhang M, Kataoka K. Nano-structured composites based on calcium phosphate for cellular delivery of therapeutic and diagnostic agents. Nano Today 2009;4:508–17.
[30] Sullivan LA, Brekken RA. The VEGF family in cancer and antibody-based strategies for their inhibition. MAbs 2010;2(2):165–75.
[31] Dvorak HF. Vascular permeability factor/vascular endothelial growth factor: a critical cytokine in tumor angiogenesis and a potential target for diagnosis and therapy. J Clin Oncol 2002;20:4368–80.
[32] Boussif O, Lezoualc'h F, Zanta MA, Mergny MD, Scherman D, Demeneix B, et al. A versatile vector for gene and oligonucleotide transfer into cells in culture and *in vivo*: polyethylenimine. Proc Natl Acad Sci U S A 1995;92:7297–301.